Chapter 2 Experiment

2.0 Preface

Since the discovery of carbon nanotubes (CNTs) in 1991, one-dimensional nanowires of elemental and compound semiconductors such as Si,[148-151] Ge,[152-153] InP,[154] GaAs[155] and SnO_2[156] have been synthesized by vapor-liquid-solid（VLS）growth mechanism,[157-159] solution-liquid-solid (SLS) growth mechanism,[160] gas-solid (GS) growth mechanism,[161] laser-assisted catalytic growth (LCG),[162] template-based synthetic approaches,[163] physical vapor deposition (PVD),[164-166] chemical vapor deposition (CVD)[167-170] and oxide-assisted nucleation.[171-172] The ability to synthesized nanometer scale control in diameter during anisotropic crystal growth while maintaining a good overall crystallinity, large quantities of high pure (contamination-free), ultra long and uniform-sized nanowires from these techniques offer exciting possibilities in fundamental and applied research.

2.1 Introduction

Since the 1964, Si whiskers were synthesized by the well-known VLS growth mechanism. In the VLS growth mechanism, metal particles such as Au, Fe, or Cu, are deposited on the Si substrate used as the mediating solvent.[84-88] The Au forms the Au droplet on the Si substrate. The liquid droplets serve as catalytic sites, which absorb the reactants on the substrate. When droplets supersaturated, the reactants in vapor phase bond to the Si substrate at the

liquid-solid interface, and the nanowires grow. The growth directions of these nanowires are decided by the lowest liquid-solid interfacial energy at the liquid-solid interface.

2.2 Synthesized of ZnO Nanowires

2.2.1 Traditional Process for Synthesized ZnO NWs

While using the VLS process to fabricate the ZnO NWs, the traditional VLS process is selected Au to be a catalyst and ZnO mixed carbon powder to be a beginner source. Then put the substrate in the furnace which heating to about 900 ^{o}C for a while. The substrate always uses sapphire which have the same crystalline of the ZnO NWs. Because of the same crystalline of sapphire and ZnO, the ZnO NWs can grow on the sapphire so directly. This fabricate method offer a easily synthesized environment which can speedy fabricate mass of the ZnO NWs but it is hard to integrated to the device level process. For improve this disadvantages, some of modified VLS process are presents as later section which offer a effectively method to lowering the lattice mismatch between substrate and ZnO NWs. Therefore, using modified VLS process that can overcome the integrated problem and also offer the well growth direction of the ZnO NWs.

2.2.2 Two-Step Vapor-Liquid-Solid (VLS) Process for Synthesized ZnO NWs

In our experiment, p-type Si (100) substrate was cleaned following the procedure adopted by Yang et. al. A thin layer of copper was deposited on the

cleaned Si (100) substrate by rf-sputtering using a copper target. The copper thin film coated on Si substrate was about 70 Å and 150 Å thicknesses, respectively. The copper-coated Si substrate was heated in a rapid thermal annealing (RTA) furnace at 900 ^{o}C for 1 hour. ZnO (99.99%, -325 mesh, Alfa Aesar) and carbon (99.99%, -325mesh, Alfa Aesar) powders were mixed, placed in a quartz boat, and loaded to the center of a tube furnace. The annealed copper/Si substrate was placed in the same boat with mixed powder. The ZnO NWs were grown with temperatures in the range 850 to 950^{o}C under flowing high purity Ar (99.998%) gas with the gas flow rates of 5.0-40.0 sccm. The synthesized samples had a gray-violet color. We introduced two heating schedules for the fabrication of ZnO NWs using VLS growth process: (i) directly increasing the growth temperature from room temperature to 850-950^{o}C, (ii) increasing the growth temperature to 800 ^{o}C, keeping the temperature constant for 6 minutes and then further increasing the growth temperature to 850-950^{o}C.

2.2.3 Deposited of the ZnO Buffer Layer

The p-type Si (100) substrate was cleaned by a standard RCA cleaning method and rinsed in acetone for 30 min. to remove native oxide from the surface of Si substrate. Subsequently, the epitaxial ZnO buffer layer was deposited by rf-sputtering (100W, 450^{o}C at 5 mtorr for 60 min.) and in-situ annealing at 450^{o}C for 30 min. After annealing, the thickness of the epitaxial ZnO buffer layer was about 100 nm, which had a dominant orientation along (002). A thin copper layer of 70 Å in thickness was deposited on ZnO (002)/Si (100) substrate by rf-sputtering under 10 mtorr pressure at 60 W power for 15

sec. The ZnO nanowires were synthesized by VLS process[12] at temperature of 750~950 ^{o}C under flowing (rates of 20.0~100.0 sccm) high purity Ar (99.998%) gas.

2.2.4 The Sn Doped ZnO NWs

To prepare the p-type Si (100) substrate for the synthesis of SZO nanowires, the substrate was cleaned by the standard Radio Corporation of America (RCA) cleaning method. After cleaning, the rf-sputtering (13.56 MHz) was adopted to deposit an ultra-thin Au catalyst film (~60 Å thick) under Ar sputtering gas (5.0 cm^3/min.) at 20 mTorr for ~10−30 sec. Our synthesis process was performed by a VLS fabrication process. The ball-milled (24 hr) and mixed powders of ZnO, SnO_2 and carbon (Alfa Aesar, 99.995%) were consisted of 0, 0.1 and 0.3 mole fractions of Sn. Then, the mixed powder was loaded into a quartz boat and placed in the center of a quartz tube. The cleaned p-Si(100) substrate was loaded in to the lower temperature region of the quartz boat. The quartz tube was laid in a horizontal furnace. The synthesis temperature of the VLS process of undoped ZnO and SZO nanowires were ~900 and ~800 ^{o}C, respectively. High purity Ar gas was used as carrier gas with the gas flow rate of 50−100 cm^3/min.

2.2.5 The Sn Doped In_2O_3 NWs

A Radio Corporation of America (RCA) cleaning method was used to clean p-type Si (100) substrate. This process can remove the native oxide (~20 Å) from the surface of Si substrate. After the cleaning procedure, the 70 Å thick

Au film with a diameter of 100 μm was formed on Si (100) substrate by rf-sputtering (13.56 MHz) under 10 mTorr Ar atmosphere at a power level of 30 W for 15s and then patterned by the shadow mask process. This Au film acts as a catalyst for SIO NWs synthesized through a precise carrier gas flow-controlled VLS process and the control of the growth region of the nanowires.

The source material for SIO NWs was a mixture of IO (99.998%), SnO_2 (99.98%), and graphite (99.98%) powders at a mole ratio of 0.9:0.1:1.0. The mixed powders were put on the quartz boat in front of the Au/Si substrate loaded in a horizontal alumina tube furnace. The SIO NWs were synthesized by the VLS process with the temperatures varying from 770 to 950 ^{o}C. The furnace was heated at a rate of 150 ^{o}C/min. under the gas flow rate of high purity N_2 (99.998%) varied from 20.0 to 100.0 cm^3/sec. The optimized gas flowing rate used in our study was 60.0 cm^3/sec. On the basis of our previous study[7], the carrier gas controlled to nearly laminar flow mode in the horizontal furnace is able to be helpful in the vertical growth of the nanowires.

2.3 Characteristics of ZnO Nanowires

After synthesized the ZnO NWs, there are a series analysis to indicate the characteristics of many kind application potentials. Typically, that can differentiate between three fields; in the first is materials analysis that knows the basic properties of the ZnO NWs, the optical properties which can go to another step to indicate the emission mechanism is second, and the characteristics of field emission which indicate the electric relationship of the ZnO NWs are the least.

2.3.1 Materials Analysis for ZnO NWs

The materials analysis are indicated that the several kinds characteristics of the ZnO NWs. Through these analysis, the crystalline, lattice structure, defects of crystalline, chemical composition, binding conditions and dopant effects can easily understand to describe the ZnO NWs.

2.3.1.1 Physical Analysis for ZnO NWs

About the physical analysis for ZnO NWs which is to determine the crystalline while the nano structure synthesized by the VLS process or others. Typically, the physical measurements such as the X-ray diffraction method which could determines the crystal structure and the information of the lattice arrangements. The field emission scanned electron microscopy (FE-SEM) rely on the higher accelerate voltage than thermal SEM which offer good resolution to analysis the geometry of the ZnO NWs. The high resolution transmission electron microscopy (HR-TEM) have the well transmission ability that can offer many information for the little selected area to observe of the ZnO NWs.

The XRD is mainly measured the crystalline of the ZnO NWs which result in the very convenient process it have and a lot of information for lattice structure. Generally, the theta-two theta method is used to analysis the intensities of the diffraction peaks. According these intensities of diffraction peaks, we can know what crystalline does the nanowires have. Typically, ZnO NWs are dominated at (002) direction which along the c-axis. The width of the diffraction peaks will indicate the similar grain size. The sharper peak means the well crystal structure for the ZnO NWs. Then, the Full-Width

Half-Maximum (FWHM) also help to indicate that the crystalline. In summary, the XRD method can offer a speedy rule to analysis the lattice structure of the ZnO NWs which help us easily to change the growth process controlled conditions. That will save more time to prepared nanowires for other analysis.

The field emission micro scanning microscopy (FE-SEM, Hitachi S-4700) is observed the appearance of the nanowires. Through the higher accelerate voltage and accurate focus ability from the FE-SEM, the geometry of the nanowires is easily measured and calculated their aspect ratio. Generally, the diameter of the ZnO NWs is in the range between ~30 nm to ~80 nm and the length of them is about 4-8 μm, respectively. On the other hands, the side wall of the ZnO NWs is very smooth. From the two step thermal heating process were introduced, the ZnO NWs don't have any metal catalyst tip remained which can pictured by the FE-SEM. Furthermore, we also can use the electrons diffraction spectra mapping (EDS) to recognize the elements which the ZnO NWs have that will help us to understand the diffuse ion mechanism while being the VLS process.

To understand the lattice structure, micro region composition, and morphology of the surface of the nanowires, high resolution transmission electron microscopy (HR-TEM, Philips tecani-20) was used to observe these nanowires. According the diameters and width of the nanowires are thin enough to let the accelerated electron beam through, the nanowires is take off from the substrate by acetone (45 %) solution. The sample is put into the acetone and use ultra wave cleaner for a while. Then, we use the TEM copper grid catch the dispersed ZnO NWs and dry the copper grid on the vacuum oven by 75 ^{o}C about 24 hrs.

The HR-TEM can get more information of the ZnO NWs which can list as

follow:

(a) Bright view images, these images are directly indicate the morphology of the ZnO NWs. Through the photograph, the growth situation of the nanowires could identify which help knowing the VLS process mechanism.

(b) Dark view images, while the electron beam was under the diffraction condition and change to one selected pole, the dark view image can have. This image can indicate fewer defects such as line defect or lattice mismatch which hided in bright view images.

(c) High resolution lattice image, these images can indicate the atom arrangement of the ZnO NWs. There are so clear lattice structure is shown which speedy observe the Zn, O, or some fewer elements including into the ZnO NWs. On the other hands, the clear lattice fringes will help to calculated the d-spacing along the c-axis which prove the crystalline.

(d) Selected area electron diffraction patterns, when the HR-TEM is under the diffraction optical path, using the SAD capture to limit the electron beam which can have the crystal diffraction patterns. Using the SAED pattern, every possible d-spaceings will be calculated by diffraction rules. After compare these lattice parameter, the crystalline of ZnO NWs is easily to identify and discuss which process made.

2.3.1.2 Chemical Analysis for ZnO NWs

To understand the chemical composition of the ZnO NWs, the fundamentals analysis will be used to precious judge the composition and what kinds of elements which the ZnO NWs have.

Firstly, the X-ray photoelectron spectroscopy (XPS) is taken to know the

binging energy between each element of the ZnO NWs. X-ray Photoelectron Spectroscopy known as XPS or ESCA (Electron Spectroscopy for Chemical Analysis) has been developed from the Fifties by Professor K. Siegbahn. The Physics Nobel Prize awarded his work in 1981. The most interesting thing with this technique is its ability to measure binding energy variations resulting from their chemical environment. For the past 20 years, this type of spectrometry emerged as a key tool in surface analysis, mainly because of two major features:

(a) Quantitative analysis and

(b) Informaion on the chemical nature and state of the detected elements.

By absorbing a photon, an atom gains an energy amount equal to hυ. It then releases an electron to regain its original stable energy state. The released electron retains all the energy from the striking photon. It can then escape from the atom, and even further from matter and kinetic energy keeps it moving. With XPS, incident photons usually carry an energy ranging from 1 to 2 KeV.

Second, the Auger electron spectroscopy (AES) is used to analysis the ZnO NWs. AES is a technique often described as more sensitive than XPS. It is partially true. In fact the difference in sensitivity is primarily due to the differences in electron kinetic energies. For example in the case of carbon, in XPS the kinetic energy is close to 1000 eV as opposed to 250 eV in AES. Because the mean free path changes with the electron kinetic energy (see IMFP grapher), the depth of analysis will be smaller in AES than in XPS in the case of a carbon containing specimen. As a matter-of-fact, the surface contamination (primarily carbon and oxygen) is a much more sensitive factor in AES. An ion etching is sometimes necessary to study surfaces with this spectroscopy.

AES is the ideal complement of XPS. Known as XAES, this technique

consists in simultaneously studying the Auger transitions from a photoelectron and the XPS lines. The Auger spectroscopy is not very sensitive to chemical environment, thus allowing here to solve indeterminations on the chemical state of certain elements. It is the case for aluminium the XPS lines of which exit with the same energy: only the Auger lines (obtained from a Mg source) solve the chemical nature of the element.

While using the HR-TEM, the electron diffraction spectra (EDS) is often being detect the elements which the ZnO NWs have. According the small focus electron beam and high accelerate voltage, the EDS spectra is very sensitive that help to easily analysis the atomic weight percentage of each elements. Typically, Zn and O signals are mainly peaks of the spectra, some less dopant such as Sn, Au, or others are very weak but still been detected. While using the calculation tools, the signal of copper need to be ignore because that is results in the TEM copper grid holder.

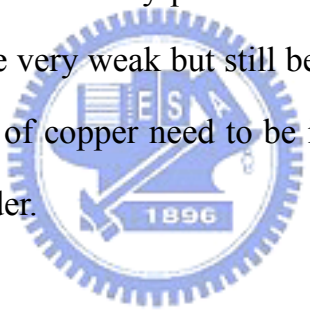

2.3.2 Photoluminescence (PL) Characteristics for ZnO NWs

Results in the wide and direct band gap of the ZnO NWs (3.37 eV), the optical emission is having much potential for nano laser application. The photoluminescence (PL) measurement can determine the properties of the optical emission of the ZnO NWs. According the different emission parks, the oxygen defect, other intersitials and vacancy effect are indicated which presents that the ZnO NWs including less impurity.

In order to realize the relationship between the impurities and the optical

characteristics, the absorption coefficient measurement was taken, and the optical band gap of the ZnO nanowires was calculated by the Tauc's[22] plot. By the Tauc's[22] equation, the optical band gap (E_g) can be determined from the intercept of $(\alpha hv)^{1/2}$ v.s. hv plot ,where α is the absorption coefficient, h is the Planck constant, and v is the frequency of radiation. As shown in Fig. 7(b), the Tauc's plot provides an estimate of the optical band gaps of these ZnO nanowires.

2.3.3 Field Emission Properties for ZnO NWs

The characteristics of field emission for the ZnO NWs are measured by the high vacuum chamber which has some feed through ports to connect the high voltage supply source such as Keithley 237 or HP DC power supply. The measurement system is controlled by the personal computer with NI Ltd., Labview® 6.1.

The Fig 2.x(a) is shown the architecture of the field emission measurement chamber. The pumping system is compose by one mechanic pump and turbo pump which can provide 300 L/s pumping ability. The pumping system could let the field emission chamber under the high vacuum which about 5×10^{-7} torr that offer the well environment for the analysis of the field emission. Furthermore, the vacuum chamber has a camera port which can in situ observe the field emission circumstance of the ZnO or other metal oxide NWs. The six electric connected terminals which also offer the extra electric analysis application are used. The precious moved changeable anode tip is moved by preciously linear motor which can move by ± 0.1 μm. On the other hand, to think about the measurement requirement, there are different types

which include different material and cross section areas of the tips could change for measured. Generally, we select one is tungsten alloy and others is copper tip that the cross section area is ~0.00709 cm^2 for field emission measurement.

2.3.4 Turn-on Electrical Field and Fowler-Nordheim Tunneling (F-N Tunneling)

The phenomenon of taking electrons from the surface of conducting materials and making them available as free electrons is called as electron

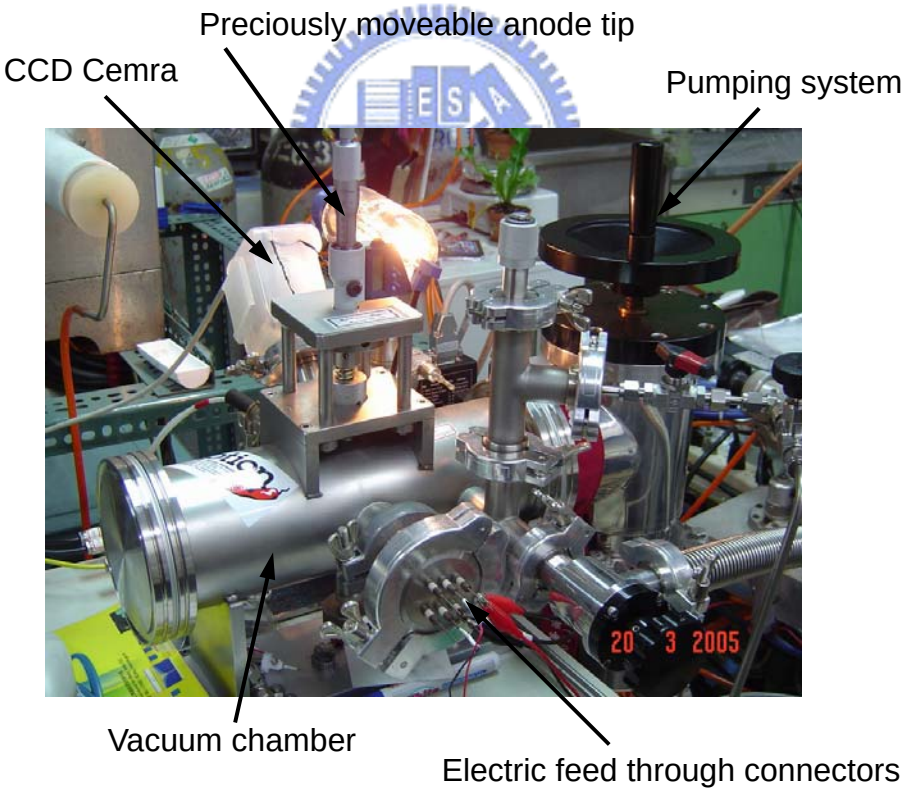

Figure 2.1 The field emission measurement system with illustration for details.

emission. The electrons can not normally escape from the surface of theconducting materials at room temperature. An extra force is exerted on them

whenever they are trying to move away from the surface. This restricting force consists of two components: one is due to the attractive force of the surface nuclei and the other is due to the image charge[173].

At a temperature of absolute 0 K, if the maximum energy of an electron in the metal is E_{max} and an electron outside the metal (at infinity) has an energy of E_o, the difference E_o and E_{max} is known as the work function E_w and is measured in electron volts. If the electrons are to escape from the metal surface, they have to have enough of energy to overcome this energy barrier. The work function therefore is the minimum energy required to allow an electron to escape from a metal at absolute 0 K.

There are four ways to enable the electrons to overcome the surface barrier and escape from the surface[174]. The four main processes are thermionic emission[175], secondary emission[176], photoelectric emission[177] and field emission[178-180]. To allow an appreciable number of electrons to overcome this potential barrier, either a sufficient energy must be given to the electrons or the hight and width of the potential barrier must be lowered by applying a strong electric field. Among these four emission processes, therminoic, photoelectric and secondary emission depend upon the energy gained by the electrons. Field emission, however, results from the reduction of the barrier height and width.

Field emission relies upon a very high electric field at the emission surface. As the electric field at the surface of a pure metal is increased, the potential barrier and the width are reduced as shown qualitatively by curve b in Fig. 2.2. The decrease in barrier width lows the electrons having energy less than E_o to tunnel through.

At room temperature the thermionic emission current is negligible. If a sufficiently along electric field is applied to the cathode surface, however, an

appreciable number of electrons at the Fermi level can tunnel through the narrow potential barrier shown by curve c in Fig. 2.2.

Electron emission caused by this strong electric field is called field emission or auto electronic emission[181-182]. Potential gradients in the order of million volts per centimeter can result in emission current densities of thousands of amperes per square centimeter. Field emission is almost independent of the emitter temperature. From wave mechanical analysis, Fowler and Nordheim derived a relationship between the field emission current density J_F from a pure metal and the electric field F[183-184].

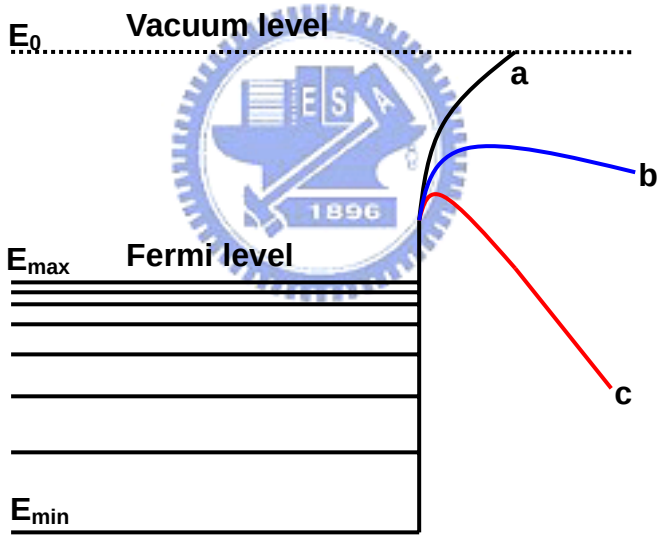

Figure 2.2 Energy band diagram showing the effect of strong electroststic field on the height of the surface potential barrier.

$$J_F = A_F F^2 \exp(-\frac{b_F}{F}) \tag{2.1}$$

Here, $A_F = \frac{q^3}{8\pi ht^2(y)E_W}$, $b_F = \frac{8\pi\sqrt{2m}E_W^{3/2}v(y)}{3hq}$

Here, v(y) and t(y) are the Nordheim elliptic functions, for which computed values are available. The Schottky lowering of the potential barrier, y, is as follow and for all practical purpose, $t^2(y)$ can be approximated by 1.1 and the approximation for $t^2(y)$ is list as:

$$y = \frac{\sqrt{\frac{qF}{4\pi\varepsilon_0}}}{E_W}, \quad v(y) = 0.95 - y^2 \tag{2.2}$$

This is surprisingly similar to the thermionic emission current equation with temperature T replaced by the field strength F. Although field emission data are difficult to explain experimentally, those existed support the F-N theory by displaying a clear relation between $\log(J_F/F^2)$ and 1/F. Millikan and his colleagues have also shown that as the temperature increases to the point where the thermionic emission begins, emission current becomes sensitive to temperature and gradually dominated by thermionic emission current. According to this observation they suggested that perhaps there exists a formula for the current density,

$$J = A(T + cF)^2 \exp(-\frac{b_F}{T + cF}) \tag{2.3}$$

This equation is valid over wide ranges of temperature (T) and field strength (F). This formula is correct for large T and small F and also for large F and small T.

Nordheim has calculated the exact reflection or emission coefficients for electrons of given energy W incident from the left of the potential barrier C as shown in Fig. 2.3(a). The problem is one dimensional. The kinetic energy W of the electron is in the direction normal to the surface of the metal. The emission coefficients of the electrons for a given energy can be calculated when a uniform external field is applied to given an energy band diagram as shown in

Fig. 2.3(b). The top of the barrier is rounded due to image force. Although this will alter the emission coefficient for the electrons with an incident energy near W, the modification is not important in calculating the field emission at ordinary temperature.

In order to study the electron tunneling mechanism through the potential barrier diagram which shown in Fig. 2.3, the wave equation needs to be rewritten as

$$\frac{d^2\Psi}{dx^2} + \kappa^2 (W - C + Fx)\Psi = 0 \qquad \text{for } x > 0 \qquad (2.4)$$

$$\frac{d^2\Psi}{dx^2} + \kappa^2 W\Psi = 0 \qquad \text{for } x < 0 \qquad (2.5)$$

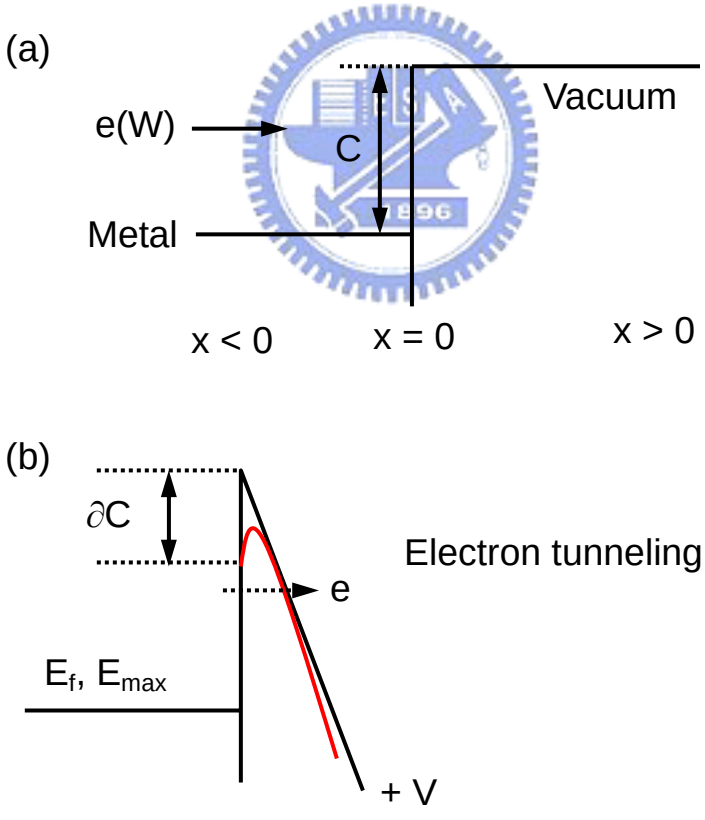

Figure 2.3 Energy band diagram showing the electron moving toward a potential barrier with (a) no external electric field, and (b) an external electric field.

subject to the boundary condition that ψ and dψ/dx are both continuous at x = 0, For x > 0, ψ represents a stream of electrons progressing to the right only. The constant κ is given by

$$\kappa^2 = 8\pi^2 m / h^2 \tag{2.5}$$

for defining a parameter u of $u = (-\frac{C-W}{F} + x)(\kappa^2 F)^{1/3}$ (2.6)

the eqn. 6.4 becomes $\frac{d^2\Psi}{dx^2} + u\Psi = 0$ (2.7)

The solutions of eqn. 2.7 are expressed in terms of Bessel's function of order

$$\Psi = \sqrt{u} J_{\pm\frac{1}{3}}(\frac{2}{3}u^{3/2}) \tag{2.8}$$

Because the solution represents a wave traveling to the right at large x,

$$\Psi = \sqrt{u} H^{(2)}_{1/3}(\frac{2}{3}u^{3/2}) \tag{2.9}$$

where $H^{(2)}$ is the second function of Hankel. For large u

$$\Psi \sim (\frac{2}{\pi})^{1/2} \frac{1}{u^{1/4}} \frac{1}{(2/3)^{1/2}} \exp(-i(\frac{2}{3}u^{3/2} - \frac{5\pi}{12})) \tag{2.10}$$

as u approaches infinite $|\Psi|^2 \sim \frac{B}{(W - C + Fx)^{1/2}} = \frac{B}{\upsilon}$ (2.11)

where B and B' are constants and υ is the velocity of the electron.

For x < 0, $\Psi = \frac{1}{W^{1/2}}[a\exp^{-i\kappa x\sqrt{W}} + a'\exp^{-i\kappa x\sqrt{W}}]$ (2.12)

There is no ambiguity that ψ is represented by a power series of integral power of u. Using the boundary condition that ψ and dψ/dx are continuous at $x = \pm 0$, one can obtain four equations involving $(\psi)_0$ and $(d\psi/dx)_0$.

Define the transmission probability D(w) as

$$D(w) = \frac{|a|^2 - |a'|^2}{|a|^2} \tag{2.13}$$

Applying the boundary condition, eqn. 6.13 becomes

$$D(w) = \frac{4(W(C-W))^{1/2}}{C} \exp(-\frac{4\kappa(C-W)^{3/2}}{3F}) \quad (2.14)$$

Nordheim also calculated the number of electrons N(w) incident on the surface per unit area and time with a kinetic energy W normal to the surface. According to Sommerfield's theory,

$$N(w) = \frac{4\pi mkT}{h^3} L(\frac{W-\mu}{kT}) \quad (2.15)$$

$$\text{here, } L(\beta) = \int_0^\infty \frac{dy}{e^{\beta+y}+1} \quad (2.16)$$

and μ is the usual parameter of the electron distribution in the Fermi-Dirac statistics equivalent to the thermodynamic partial potential of an electron. Hence the current density J (amp/cm^2) is given generally by

$$J = \int_0^\infty D(w)N(w)dw \quad (2.17)$$

Substituting in the equations for D(w) and N(w), eqn. 2.17 can be expressed as

$$J = \frac{4\pi mqkT}{h^3} \int_0^\infty D(w)L(\frac{W-\mu}{kT})dw \quad (2.18)$$

or simplified as

$$J = \frac{q}{2\pi h} \frac{\mu^{1/2}}{C(C-\mu)^{1/2}} F^2 \exp(-\frac{4\kappa(C-\mu)^{3/2}}{3F}) \quad (2.19)$$

A typical Fowler-Nordheim plot is shown in Fig. 2.4. It shows a linear curve if lon(I/V^2) is plotted versus 1/V.

2.4 Summary

In summary, many of fabrication processes and analysis methods are help us to study the ZnO NWs. The Cu catalyzed VLS process, which offer good thermal process control, less contamination and precise chemical composition,

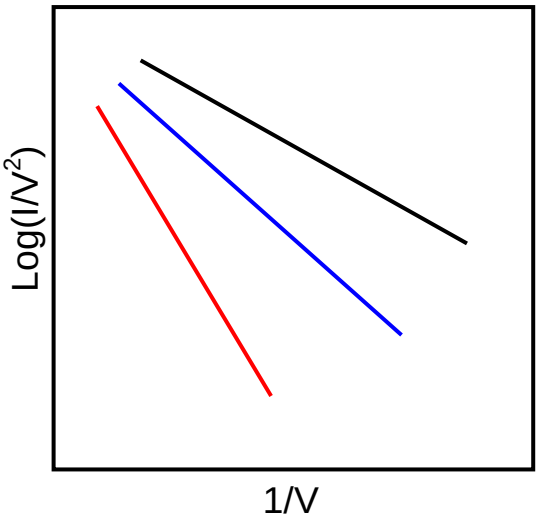

Figure 2.4 Fowler-Nordheim plot of the current-voltage characteristic of a typical nanowires at room temperature.

The modified VLS process which effectively present the well crystalline and better growth direction of ZnO NWs.

The optical emitted and band energy study are offer the references in the optical field of the ZnO NWs. The field emission analysis also helps to determine the potential of the flat display of the ZnO NWs.